

# Robust Lane Detection with Wavelet-Enhanced Context Modeling and Adaptive Sampling

Kunyang Li and Ming Hou

Faculty of Information Engineering and Automation  
Kunming University of Science and Technology  
No. 727, Jingming South Road, Chenggong District, Kunming City, Yunnan 650500,  
P. R. China  
2197569331@qq.com

**Abstract.** Lane detection is critical for autonomous driving and advanced driver assistance systems (ADAS). While recent methods like CLRNet achieve strong performance, they struggle under adverse conditions such as extreme weather, illumination changes, occlusions, and complex curves. We propose a Wavelet-Enhanced Feature Pyramid Network (WE-FPN) to address these challenges. A wavelet-based non-local block is integrated before the feature pyramid to improve global context modeling, especially for occluded and curved lanes. Additionally, we design an adaptive preprocessing module to enhance lane visibility under poor lighting. An attention-guided sampling strategy further refines spatial features, boosting accuracy on distant and curved lanes. Experiments on CULane and TuSimple demonstrate that our approach significantly outperforms baselines in challenging scenarios, achieving better robustness and accuracy in real-world driving conditions.

**Keywords:** Lane Detection · Multi-Scale Fusion · Feature Pyramid Network (FPN) · Wavelet Convolution.

## 1 Introduction

Lane detection is a fundamental task in autonomous driving and Advanced Driver Assistance Systems (ADAS), providing essential cues for vehicle localization, path planning, and steering control. Accurate lane perception enables vehicles to maintain lane discipline and make informed navigation decisions, contributing significantly to driving safety and system robustness. With the rapid development of deep learning, lane detection methods have shifted from traditional handcrafted features to learning-based models, achieving remarkable progress in both accuracy and efficiency.

Recent deep models for lane detection can be broadly categorized into three paradigms: segmentation-based, anchor-based, and curve-based approaches. Segmentation methods [9,24,27] formulate lane detection as a pixel-wise classification task. Despite their strong capability in capturing detailed lane structures,

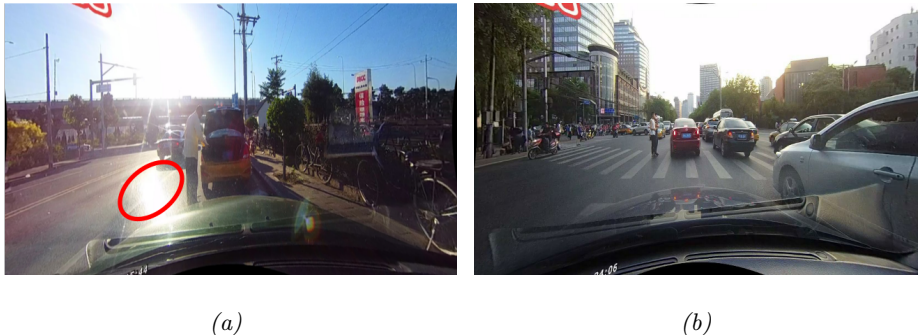


**Fig. 1.** Illustrations of hard cases for lane detection. (a) The case that lane is blurred by the extreme lighting condition. (b) The road with complex paths.

these methods suffer from high computational overhead and are sensitive to complex scenes with occlusions, shadows, and extreme lighting. Anchor-based methods [7] regress lane positions by predicting anchor points or anchor lines but often struggle with curved lanes or scenarios involving severe occlusion and illumination changes. Curve-based models [21,25] directly predict curve parameters to fit lane markings, reducing computational cost, yet they face difficulties handling complex road geometries or multiple lane scenarios.

While recent advances such as CLRNet [2] have introduced powerful feature aggregation modules and optimized training strategies, robust lane detection under adverse conditions—including heavy rain, snow, glare, and occlusion—remains a challenging problem. Inspired by the success of non-local operations in capturing long-range dependencies and recent advancements in multi-scale feature modeling [23,6], we propose a Wavelet-Enhanced Feature Pyramid Network (WE-FPN) to address these limitations. Specifically, we incorporate a wavelet-enhanced non-local module to better capture contextual dependencies and design an adaptive preprocessing module for illumination enhancement. Furthermore, an attention-guided sampling strategy is introduced to refine long-range spatial features, particularly improving curved lane detection.

Our contributions are summarized as follows:

- We propose WE-FPN, a wavelet-enhanced feature pyramid network that effectively integrates multi-scale contextual information to improve lane detection under challenging conditions.
- An adaptive preprocessing module is designed to enhance image quality in extreme lighting scenarios, boosting lane visibility and feature representation.
- We introduce an attention-guided sampling strategy to emphasize long-range structural cues, significantly improving curved and distant lane detection.

Experiments on CULane [12] and TuSimple [22] benchmarks demonstrate that our method achieves state-of-the-art performance, especially in complex scenes such as occlusion, curved lanes, and low-light environments.

## 2 Related Work

### 2.1 Deep Learning-based Lane Detection

Deep learning has revolutionized lane detection by enabling end-to-end feature learning and robust modeling of complex road scenes. Segmentation-based methods treat lane detection as a pixel-wise classification problem, enabling detailed localization of lane regions. SCNN [12] pioneers spatial message passing to enhance the continuity of lane predictions, while RESA [27] further improves contextual aggregation through learnable recurrent shifts. Despite their effectiveness, these methods suffer from high computational cost and poor generalization under occlusion and complex backgrounds. Anchor-based approaches predict predefined anchors or row-wise lane positions. LaneATT [20] and SGNet [19] leverage structured attention and vanishing point constraints to enhance anchor regression. UFLD [14] and CondLaneNet [9] focus on efficiency by adopting row-wise anchors and conditional convolutions. However, such methods often rely heavily on start-point localization and struggle with curved or heavily occluded lanes. Curve-based models, including PolyLaneNet [21], model lane markings as parametric curves, offering computational efficiency and compact representations. Yet, fitting complex lane topologies remains challenging, especially in multi-lane or high-curvature scenarios.

### 2.2 Feature Enhancement and Context Modeling

Recent works highlight the importance of multi-scale feature fusion and long-range context modeling in visual tasks. For instance, Weng et al. [23] propose selective frequency interaction networks to enhance aerial object detection, demonstrating the effectiveness of adaptive feature selection. Similarly, Li et al. [6] introduce LR-FPN for remote sensing object detection, refining feature pyramids with location-sensitive enhancement. Inspired by these advancements, our work integrates wavelet-based non-local modeling into lane detection to enhance global context capture while preserving fine-grained lane features. Additionally, our attention-guided sampling strategy draws inspiration from recent progress in human-centric generation tasks, where adaptive feature modulation significantly improves generation fidelity [18,16,17]. Despite significant progress, robust lane detection under challenging conditions remains difficult. Variations in lighting, road markings, occlusions, and weather significantly degrade detection performance. CLRNet [2] addresses some of these challenges by introducing RoIGather and SimOTA to improve context aggregation and label assignment. However, detection-based methods still rely on heavy post-processing and struggle with global consistency.

## 3 Approach

### 3.1 Data Preprocessing

**Motivation.** Although CLRNet[2] has shown enhanced robustness in handling challenging environmental conditions such as heavy rain, snow, occlusions, and

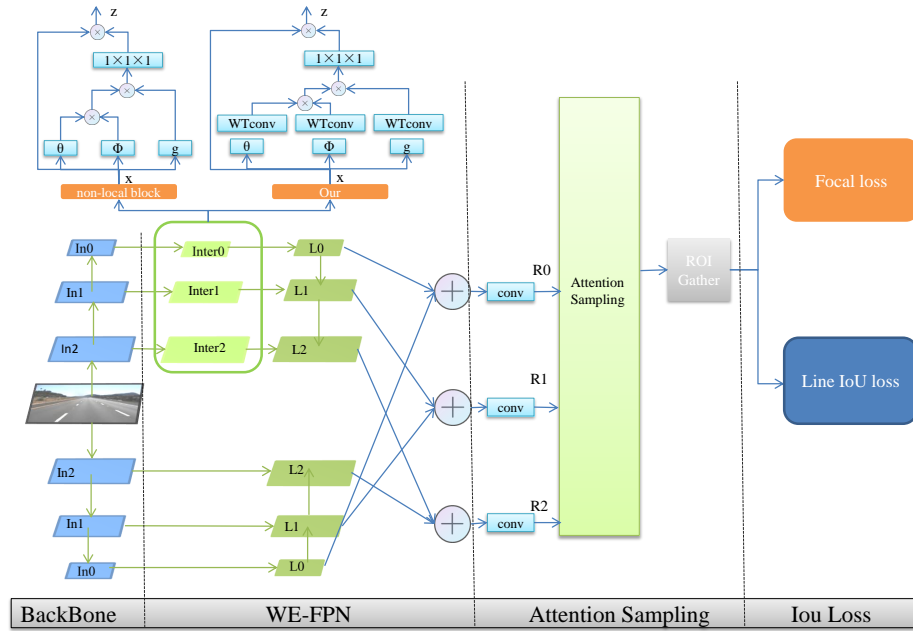


**Fig. 2.** Overview of the proposed **our**. (a) The network generates feature maps from WE-FPN structure. Subsequently, each lane prior will be refined from high-level features to low-level features. (b) The input layers feed into internal layers integrated with positional non-local blocks to capture spatial context. (c) The internal layers connect to output layers that pass through Attention Sampling.

intense illumination, its performance still falls short of optimal when faced with severe environmental distortions. A significant limitation stems from the degradation in image quality caused by these adverse scenarios, which significantly complicates the extraction of lane features. To overcome this challenge, we introduce an innovative adaptive preprocessing pipeline designed to dynamically adjust and optimize image brightness and contrast, thereby enhancing lane visibility and reducing the ambiguity of features for subsequent detection models.

The proposed pipeline processes the input image through a sophisticated two-stage enhancement workflow. In the first stage, a histogram analysis module meticulously examines the image to identify regions that are either overexposed or underexposed. Following this, an adaptive gamma correction technique is applied to standardize the overall brightness of the image, effectively addressing extreme lighting variations such as glare or low-light conditions. In the second stage, a hybrid contrast enhancement algorithm is employed, which integrates CLAHE (Contrast-Limited Adaptive Histogram Equalization) with guided filtering. This combination not only sharpens the details of lane edges but also

effectively suppresses noise amplification in uniform areas, ensuring a clearer and more accurate representation of lane features for downstream processing.

### 3.2 Wavelet-Enhanced FPN (WE-FPN)

To tackle the limitations of CLLNet’s Feature Pyramid Network (FPN) in effectively extracting local features, particularly in scenarios involving occlusions and crowded environments, as illustrated in Fig. 2, we introduce a novel Wavelet-Enhanced FPN (WE-FPN) architecture. This advanced framework incorporates an enhanced non-local block that is further augmented with wavelet convolution, a technique that significantly improves feature representation. Specifically, the discrete wavelet transform is employed to decompose input features into high-frequency subbands, which capture fine-grained details such as lane textures, and low-frequency subbands, which preserve structural and global topological information. This multi-scale decomposition process allows the model to explicitly and simultaneously capture both intricate local details and broader structural coherence, addressing the shortcomings of traditional FPNs in complex scenarios.

Additionally, to ensure seamless integration of the enhanced features, we propose a weighted fusion mechanism that intelligently combines the outputs from the original FPN branch and the wavelet-enhanced branch. This fusion mechanism is carefully designed to balance the contributions of both branches, leveraging the strengths of each to produce a more robust feature representation. Following the fusion step, a  $3\times 3$  convolution layer is applied to refine the aggregated features and suppress any potential aliasing artifacts that may arise from the multi-scale aggregation process. This refinement ensures that the final feature maps are both precise and artifact-free, thereby improving the overall performance of the lane detection model in challenging environments. By integrating wavelet-based multi-scale analysis and a sophisticated fusion strategy, the WE-FPN architecture significantly enhances the model’s ability to handle occlusions, crowded scenes, and other complex scenarios, ultimately leading to more accurate and reliable lane detection.

### 3.3 Attention Sampling

**Motivation.** The uniform sampling strategy employed in CLRNet inadequately addresses the importance of vanishing points in distant regions, leading to sub-optimal performance in predicting curved lanes. To mitigate this limitation, we propose an attention-guided sampling mechanism inspired by spatial attention principles. Instead of treating all regions equally, this approach dynamically prioritizes regions containing critical geometric cues (e.g., vanishing points and curvature transitions) while suppressing less informative areas. As illustrated in Fig. 3, the proposed sampling strategy retains high-confidence predictive features and semantic cues essential for robust lane geometry inference, particularly enhancing curvature estimation accuracy. By aligning feature aggregation with lane

topology priors, the method achieves significant improvements in both structural coherence and detection precision for complex road geometries.

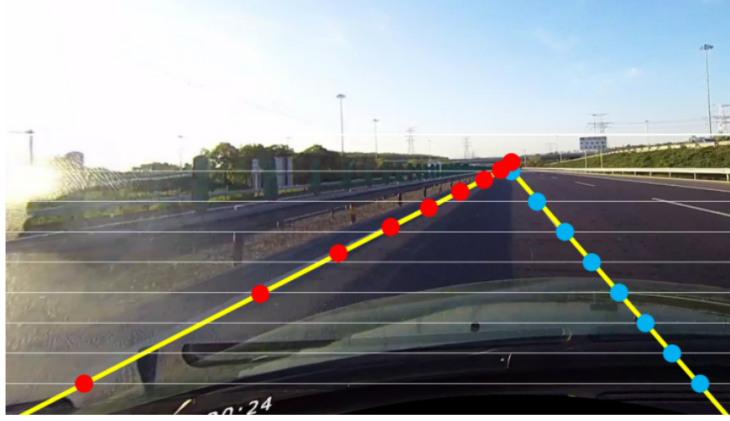


**Fig. 3.** Visual depiction comparing **Attention Sampling** (red dots) versus **uniform sampling** (blue dots).

The formula for this Attention Sampling is:

$$y = \frac{H}{N_{sample} - 1} * \log_{feature} a_n. \quad (1)$$

The term  $a_n = \frac{1}{N_{sample}-1} * i$  represents an arithmetic sequence scaling from 0 to 1 across  $i$  data points, where  $N_{sample}$  is the number of sample points and  $H$  is the image height. To generate focusing sample points, the feature point distribution undergoes a logarithmic transformation, converting feature points into integer sample values. This method emphasizes the extraction of key semantic information. Due to the possibility of repeated values from logarithmic discretization, deduplication is applied in post-processing.

### 3.4 Training and Inference Details

**Positive samples selection.** During the training process, each ground truth lane is dynamically matched with one or more predicted lanes as positive samples, following the methodology inspired by [3]. Specifically, we rank the predicted lanes according to a predefined assignment cost metric, which is formulated as follows:

$$\begin{aligned} \mathcal{C}_{assign} &= w_{sim}\mathcal{C}_{sim} + w_{cls}\mathcal{C}_{cls}, \\ \mathcal{C}_{sim} &= (\mathcal{C}_{dis} \cdot \mathcal{C}_{xy} \cdot \mathcal{C}_{theta})^2. \end{aligned} \quad (2)$$

Here  $\mathcal{C}_{cls}$  is the focal cost[8] between predictions and labels.  $\mathcal{C}_{sim}$  is the similarity cost between predicted lanes and ground truth. It consists of three parts,  $\mathcal{C}_{dis}$  means the average pixel distance of all valid lane points,  $\mathcal{C}_{xy}$  means the distance of start point coordinates,  $\mathcal{C}_{theta}$  means the difference of the theta angle, they are all normalized to  $[0, 1]$ .  $w_{cls}$  and  $w_{sim}$  are weight coefficients of each defined component. Each ground truth lane is assigned with a dynamic number (top-k) of predicted lanes based on  $\mathcal{C}_{assign}$ .

**Training Loss.** The training loss comprises two components: classification loss and regression loss. Notably, the regression loss is computed exclusively for the assigned positive samples. The overall loss function is formulated as follows:

$$\mathcal{L}_{total} = w_{cls}\mathcal{L}_{cls} + w_{xytl}\mathcal{L}_{xytl} + w_{LIoU}\mathcal{L}_{LIoU}. \quad (3)$$

$\mathcal{L}_{cls}$  is the focal loss between predictions and labels,  $\mathcal{L}_{xytl}$  is the smooth- $l_1$  loss for the start point coordinate, theta angle and lane length regression,  $\mathcal{L}_{LIoU}$  is the Line IoU loss between the predicted lane and ground truth. Optionally, we can add an auxiliary segmentation loss following[14]. It is only used in the training period and has no cost in inference.

**Inference.** To filter out background lanes (low-score lane priors), we apply a classification score threshold. Additionally, we employ Non-Maximum Suppression (NMS) to eliminate highly overlapping lanes, following the approach in [20]. Notably, our method can operate without NMS by adopting a one-to-one assignment strategy, i.e., setting the top-k value to 1.

## 4 Experiment

We evaluate our method on two widely used lane detection benchmarks: **CULane** [12] and **TuSimple** [22].

**CULane** [12] is a large-scale dataset designed for complex urban driving scenarios. It contains 100,000 images ( $1640 \times 590$  resolution) covering nine challenging categories, including crowded scenes, night, and crossroad conditions. The dataset provides rich annotations to benchmark lane detection performance under diverse real-world environments.

**TuSimple** [22] focuses on highway driving scenes, providing 6,408 images ( $1280 \times 720$  resolution) split into 3,268 training, 358 validation, and 2,782 test images. Its clean annotations and controlled scenarios make it a standard benchmark for evaluating lane detection accuracy in highway settings.

### 4.1 Implementation details

Primarily, DLA34[26] and ResNet [4] are used as the backbone network for pre-training in this study. Under the backbone network, the CULane dataset is set

**Table 1.** State-of-the-art results on CULane. In addition, we also evaluation these detectors to report the mF1, F1@50, F1@75. For “Cross” category , only false positives are shown. The reported metric of these categories is based on F1@50.

Method	Backbone	mF1	F1@50	F1@75	Normal	Crowded	Dazzle	Shadow	No line	Arrow	Curve	Cross	Night
SCNN [12]	VGG16	38.84	71.60	39.84	90.60	69.70	58.50	66.90	43.40	84.10	64.40	1990	66.10
RESA [27]	ResNet34	-	74.50	-	91.90	72.40	66.50	72.00	46.30	88.10	68.60	1896	69.80
RESA [27]	ResNet50	47.86	75.30	53.39	92.10	73.10	69.20	72.80	47.70	88.30	70.30	1503	69.90
FastDraw [13]	ResNet50	-	-	-	85.90	63.60	57.00	69.90	40.60	79.40	65.20	7013	57.80
E2E [25]	ERFNet	-	74.00	-91.00	73.10	64.50	74.10	46.60	85.80	71.90	2022	67.90	
UFLD [14]	ResNet18	38.94	68.40	40.01	87.70	66.00	58.40	62.80	40.20	81.00	57.90	1743	62.10
UFLD [14]	ResNet34	-	72.30	-	90.70	70.20	59.50	69.30	44.40	85.70	69.50	2037	66.70
PINet [5]	Hourglass	46.81	74.40	51.33	90.30	72.30	66.30	68.40	49.80	83.70	65.20	1427	67.70
LaneATT [20]	ResNet18	47.35	75.13	51.29	91.17	72.71	65.82	68.03	49.13	87.82	63.75	<b>1020</b>	68.58
LaneATT [20]	ResNet34	49.57	76.68	54.34	92.14	75.03	66.47	78.15	49.39	88.38	67.72	1330	70.72
LaneATT [20]	ResNet122	51.48	77.02	57.50	91.74	76.16	69.47	76.31	50.46	86.29	64.05	1264	70.81
LaneAF [1]	ERFNet	48.60	75.63	54.53	91.10	73.32	69.71	75.81	50.62	86.86	65.02	1844	70.90
LaneAF [1]	DLA34	50.42	77.41	56.79	91.80	75.61	71.78	79.12	51.38	86.88	72.70	1360	73.03
SGNet [19]	ResNet18	-	76.12	-	91.42	74.05	66.89	72.17	50.16	87.13	67.02	1164	70.67
SGNet [19]	ResNet34	-	77.27	-	92.07	75.41	67.75	74.31	50.90	87.97	69.65	1373	72.69
FOLOLane [15]	ERFNet	-	78.80	-	92.70	77.80	75.20	79.30	52.10	89.00	69.40	1569	74.50
CondLane [9]	ResNet18	51.84	78.14	57.42	92.87	75.79	70.72	80.01	52.39	89.37	72.40	1364	73.23
CondLane[9]	ResNet34	53.11	78.74	59.39	93.38	77.14	71.17	79.93	51.85	89.89	73.88	1387	73.92
CondLane[9]	ResNet101	54.83	79.48	61.23	93.47	77.44	70.93	80.91	54.13	90.16	75.21	1201	74.80
CLRNet[2]	ResNet18	55.23	79.58	62.21	93.30	78.33	73.71	79.66	53.14	90.25	71.56	1321	75.11
CLRNet[2]	ResNet34	55.14	79.73	62.11	93.49	78.06	74.57	79.92	54.01	90.59	72.77	1216	75.02
CLRNet[2]	DLA34	<b>55.64</b>	<b>80.47</b>	62.78	93.73	79.59	<b>75.30</b>	<b>82.51</b>	<b>54.58</b>	<b>90.62</b>	74.13	1155	75.37
<b>(ours)</b>	ResNet18	55.23	79.57	62.21	93.40	78.30	73.22	80.25	52.97	90.17	71.56	1321	74.87
<b>(ours)</b>	DLA34	55.50	80.10	<b>63.30</b>	<b>93.50</b>	<b>79.90</b>	75.10	82.33	54.40	90.49	<b>74.71</b>	1155	<b>76.02</b>

to iterate for 15 epochs while Tusimple is set to 70. In the optimizing process, we use AdamW [11] optimizer with an initial learning rate of 1e-3 and cosine decay learning rate strategy [10] with power set to 0.9. Our network is implemented based on Pytorch with 1GPU to run all the experiments. We set the number points of lane prior  $N = 72$ , and the sampled number  $N_p = 36$ .

## 4.2 Comparison with the state-of-the-art results

**Performance on CULane.** We present the performance evaluation of our proposed method on the CULane lane detection benchmark dataset, a widely recognized and challenging dataset for lane detection tasks, and provide a comprehensive comparison with several state-of-the-art lane detection methods. As demonstrated in Table 1, our method achieves impressive results across various challenging scenarios, with an F1 score of 79.90 in crowded scenes, 74.71 in curved lanes, and 76.02 in nighttime conditions. These results not only underscore the effectiveness of our approach but also highlight its superiority over CLRNet, one of the leading methods in the field. Specifically, our method surpasses CLRNet by a margin of 0.31 in crowded scenes, 0.65 in curved lanes, and 0.03 in nighttime conditions. These improvements are particularly significant, as they demonstrate the model’s enhanced robustness and reliability in scenarios where visual evidence is often limited or ambiguous, such as low-light nighttime environments, densely crowded roads, and complex curved lane structures.



The notable improvement of 0.65 in curved lane detection is especially noteworthy, as curves are inherently more challenging due to their varying shapes and the difficulty in maintaining consistent feature extraction. This performance gain underscores the ability of our method to handle intricate and dynamic lane geometries more effectively than existing approaches. Overall, these results validate the strength of our method in addressing the limitations of current lane detection systems, particularly in challenging and real-world driving conditions, and highlight its potential for practical applications in autonomous driving and advanced driver-assistance systems (ADAS).

**Table 2.** State-of-the-art results on TuSimple. Additionally, F1 was computed using the official source code.

Method	Backbone	F1 (%)	Acc (%)	FP (%)	FN (%)
SCNN [12]	VGG16	95.97	96.53	6.17	<b>1.80</b>
RESA [27]	ResNet34	96.93	96.82	3.63	2.48
PolyLaneNet [21]	EfficientNetB0	90.62	93.36	9.42	9.33
E2E [25]	ERFNet	96.25	96.02	3.21	4.28
UFLD[14]	ResNet18	87.87	95.82	19.05	3.92
UFLD[14]	ResNet34	88.02	95.86	18.91	3.75
LaneATT[20]	ResNet18	96.71	95.57	3.56	3.01
LaneATT[20]	ResNet34	96.77	95.63	3.53	2.92
LaneATT[20]	ResNet122	96.06	96.10	5.64	2.17
FOLOLane[15]	ERFNet	96.59	<b>96.92</b>	4.47	2.28
CondLaneNet[9]	ResNet18	97.01	95.48	2.18	3.80
CondLaneNet[9]	ResNet34	96.98	95.37	2.20	3.82
CLRNet[2]	ResNet18	<b>97.89</b>	96.84	2.28	1.92
CLRNet[2]	ResNet34	97.82	96.87	2.27	2.08
CLRNet[2]	ResNet101	97.62	96.83	2.37	2.38
<b>ours</b>	ResNet18	97.70	96.66	<b>2.12</b>	2.42

**Performance on Tusimple.** Table 2 provides a detailed performance comparison between our proposed method and several state-of-the-art approaches on the CULane dataset, highlighting the competitive nature of the lane detection task. The results reveal that the performance gap among the top-performing methods is relatively narrow, indicating that the dataset may already be approaching a saturation point, where further improvements are increasingly challenging to achieve due to the already high baseline performance. Despite this, our method

achieves a notable improvement over the previous state-of-the-art, surpassing it by a margin of 0.06% in the False Positive (FP) score. This seemingly small yet statistically significant enhancement underscores the effectiveness and precision of our approach, particularly in handling some of the most challenging aspects of lane detection.

The improvement in the FP score is especially meaningful, as it reflects our method’s ability to reduce false detections while maintaining high accuracy, a critical requirement for real-world applications. This advancement demonstrates the robustness of our method in detecting lanes under a variety of difficult conditions, including curved lanes, which are inherently more complex due to their dynamic shapes, as well as scenarios involving blurred or occluded lanes and complex backgrounds. These conditions often pose significant challenges for traditional lane detection systems, leading to increased errors. However, our method’s ability to outperform existing approaches in these areas highlights its superior feature extraction capabilities and adaptability to diverse and challenging environments.

This performance gain not only validates the effectiveness of our proposed techniques but also emphasizes their potential for practical deployment in autonomous driving systems and advanced driver-assistance systems (ADAS), where accurate and reliable lane detection is crucial for ensuring safety and operational efficiency. By addressing key limitations in current methods, our approach sets a new benchmark for lane detection performance, paving the way for further advancements in the field.

### 4.3 Ablation study

To validate the effectiveness of the individual components of the proposed method, we conducted a series of comprehensive experiments on the widely used CU-Lane dataset, which encompasses diverse driving scenarios such as crowded urban roads, curved lanes, and low-light nighttime conditions. These experiments demonstrate the performance improvements achieved by each component, including the data preprocessing pipeline, attention sampling mechanism, and Wavelet-Enhanced FPN, highlighting their contributions to enhancing lane detection accuracy and robustness across challenging environments.

**Table 3.** Effects of each component in our method. Results are reported on CULane.

Data Preprocessing	Attention Sampling	WE-FPN	Crowded	Curve	Night
			79.59	74.13	75.37
✓			79.62	74.17	75.41
✓	✓		79.79	74.50	75.82
✓	✓	✓	<b>79.90</b>	<b>74.71</b>	<b>76.02</b>

**Overall Ablation Study.** To analyze the importance of each proposed method, we report the overall ablation studies in Table 3. We gradually add Data Pre-processing, Attention Sampling and WE-FPN on the DLA34 baseline. Data Pre-processing improves f1 by 0.3% 0.4% 0.4% , Attention Sampling improves f1 by 0.17% 0.33% 0.41%, WE-FPN improves f1 by 0.11% 0.21% 0.20% in Crowded, Curve and Night.

**Analysis for Data Pre-processing.** The data pre-processing module demonstrates a consistent and significant performance boost across all scenarios, with the most notable improvements in the Curve and Night scenarios (0.4% each). This suggests that data pre-processing plays a critical role in enhancing the model’s ability to handle complex and challenging environments. Potential pre-processing techniques, such as data augmentation, noise reduction, or illumination normalization, likely help the model learn more robust and generalizable features. For instance, in the Night scenario, pre-processing might involve adjusting for low-light conditions or enhancing contrast, which directly improves the model’s performance in such challenging settings. The uniform improvement across scenarios indicates that data pre-processing is a foundational step that benefits the model regardless of the specific environmental conditions.

**Analysis of Attention Sampling.** The attention sampling module shows the most significant improvement in the Night scenario (0.41%), indicating its effectiveness in low-light or complex lighting conditions. This suggests that the attention mechanism helps the model focus on the most relevant regions of the input, which is particularly beneficial when visibility is poor or when the scene contains distracting elements. In the Curve scenario, the improvement (0.33%) is also notable, likely because the attention mechanism aids in identifying key features along curved paths or irregular structures. However, in the Crowded scenario, the improvement is relatively smaller (0.17%), possibly because the dense distribution of objects makes it harder for the attention mechanism to isolate specific targets. Overall, attention sampling proves to be a powerful tool for enhancing feature extraction, especially in scenarios with challenging visual conditions.

**Analysis of WE-FPN.** The WE-FPN module provides moderate but consistent improvements across all scenarios, with the most noticeable gains in the Curve and Night scenarios (0.21% and 0.20%, respectively). This indicates that the weighted feature fusion mechanism of WE-FPN enhances the model’s ability to handle multi-scale objects and complex spatial relationships, which are common in curved roads and nighttime environments. For example, in the Curve scenario, WE-FPN likely improves the detection of objects at varying distances and orientations, while in the Night scenario, it helps integrate features from different scales to better handle low-visibility conditions. In the Crowded scenario, the improvement is smaller (0.11%), potentially because the dense and overlapping objects reduce the effectiveness of multi-scale feature fusion. Nevertheless,

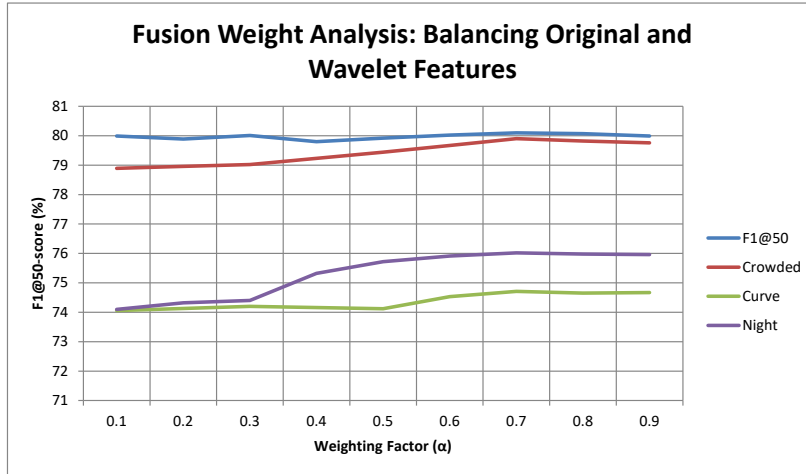


**Fig. 4.** Ablation study on the weighted combination of WE-FPN and FPN, where the contribution of WE-FPN is controlled by the weighting factor  $\alpha$  (ranging from 0.1 to 0.9). The results are computed as  $\text{WE-FPN} \cdot \alpha + \text{FPN} \cdot (1-\alpha)$ , demonstrating the impact of varying the influence of WE-FPN on model performance across different scenarios.

WE-FPN contributes to the model’s robustness by enabling more effective feature aggregation across different levels of the network.

**Ablation study on Optimal Weighting Factor.** As show in Fig. 4, the experimental results demonstrate that the proposed weighted fusion mechanism achieves optimal performance at  $\alpha = 0.7$ , where the WE-FPN branch (wavelet-enhanced features) contributes 70% and the original FPN branch contributes 30%. This balanced weighting effectively combines high-frequency details (extracted by wavelet decomposition) with low-frequency structural information (preserved by FPN), leading to significant improvements in complex scenarios such as crowded, curved, and night conditions. Specifically, at  $\alpha = 0.7$ , the model excels in capturing fine-grained textures in crowded scenes, maintaining global topological coherence in curved lanes, and enhancing edge detection under low illumination. These findings highlight the importance of the weighted fusion mechanism in balancing multi-scale features, ultimately improving the robustness and accuracy of lane detection in challenging environments.

## 5 Conclusion

This paper presents a unified lane detection framework that enhances robustness and accuracy under challenging conditions. We propose three key innovations: a preprocessing module for illumination normalization, an attention-guided sampling mechanism focusing on vanishing points and curved regions, and a Wavelet-Enhanced Feature Pyramid Network (WE-FPN) for multi-scale feature aggregation. Extensive experiments on CULane and TuSimple benchmarks demonstrate that our method outperforms the state-of-the-art CLRNet, achieving a 0.58% F1-score improvement on curved lanes while maintaining real-time efficiency (under 5ms per frame). The proposed framework effectively balances fine-grained localization and global context modeling, showing strong generalization across diverse road and lighting conditions. Future work will explore multi-modal sensor fusion and dynamic lane topology prediction to further enhance system robustness for autonomous driving applications.

## References

1. Abualsaud, H., Liu, S., Lu, D., Situ, K., Rangesh, A., Trivedi, M.M.: Laneaf: Robust multi-lane detection with affinity fields. arXiv preprint arXiv:2103.12040 (2021)
2. et al., Z.: Clrnet: Cross layer refinement network for lane detection (2022)
3. Ge, Z., Liu, S., Wang, F., Li, Z., Sun, J.: Yolox: Exceeding yolo series in 2021. arXiv preprint arXiv:2107.08430 (2021)
4. He, K., Zhang, X., Ren, S., Sun, J.: Deep residual learning for image recognition. In: Proceedings of the IEEE conference on computer vision and pattern recognition. pp. 770–778 (2016)
5. Ko, Y., Lee, Y., Azam, S., Munir, F., Jeon, M., Pedrycz, W.: Key points estimation and point instance segmentation approach for lane detection. IEEE Transactions on Intelligent Transportation Systems (2021)
6. Li, H., Zhang, R., Pan, Y., Ren, J., Shen, F.: Lr-fpn: Enhancing remote sensing object detection with location refined feature pyramid network. arXiv preprint arXiv:2404.01614 (2024)
7. Li, X., Li, J., Hu, X., Yang, J.: Line-cnn: End-to-end traffic line detection with line proposal unit. IEEE Transactions on Intelligent Transportation Systems **21**(1), 248–258 (2019)
8. Lin, T.Y., Goyal, P., Girshick, R., He, K., Dollár, P.: Focal loss for dense object detection. In: Proceedings of the IEEE international conference on computer vision. pp. 2980–2988 (2017)
9. Liu, L., Chen, X., Zhu, S., Tan, P.: Conclanenet: a top-to-down lane detection framework based on conditional convolution. arXiv preprint arXiv:2105.05003 (2021)
10. Loshchilov, I., Hutter, F.: Sgdr: Stochastic gradient descent with warm restarts. arXiv preprint arXiv:1608.03983 (2016)
11. Loshchilov, I., Hutter, F.: Decoupled weight decay regularization. In: International Conference on Learning Representations (2018)
12. Pan, X., Shi, J., Luo, P., Wang, X., Tang, X.: Spatial as deep: Spatial cnn for traffic scene understanding. In: Thirty-Second AAAI Conference on Artificial Intelligence (2018)

13. Pillion, J.: Fastdraw: Addressing the long tail of lane detection by adapting a sequential prediction network. In: Proceedings of the IEEE/CVF Conference on Computer Vision and Pattern Recognition. pp. 11582–11591 (2019)
14. Qin, Z., Wang, H., Li, X.: Ultra fast structure-aware deep lane detection. In: Computer Vision–ECCV 2020: 16th European Conference, Glasgow, UK, August 23–28, 2020, Proceedings, Part XXIV 16. pp. 276–291. Springer (2020)
15. Qu, Z., Jin, H., Zhou, Y., Yang, Z., Zhang, W.: Focus on local: Detecting lane marker from bottom up via key point. In: Proceedings of the IEEE/CVF Conference on Computer Vision and Pattern Recognition. pp. 14122–14130 (2021)
16. Shen, F., Jiang, X., He, X., Ye, H., Wang, C., Du, X., Li, Z., Tang, J.: Imagdressing-v1: Customizable virtual dressing. arXiv preprint arXiv:2407.12705 (2024)
17. Shen, F., Shu, X., Du, X., Tang, J.: Pedestrian-specific bipartite-aware similarity learning for text-based person retrieval. In: Proceedings of the 31th ACM International Conference on Multimedia (2023)
18. Shen, F., Tang, J.: Imagpose: A unified conditional framework for pose-guided person generation. In: The Thirty-eighth Annual Conference on Neural Information Processing Systems (2024)
19. Su, J., Chen, C., Zhang, K., Luo, J., Wei, X., Wei, X.: Structure guided lane detection. arXiv preprint arXiv:2105.05403 (2021)
20. Tabelini, L., Berriel, R., Paixao, T.M., Badue, C., De Souza, A.F., Oliveira-Santos, T.: Keep your eyes on the lane: Real-time attention-guided lane detection. In: Proceedings of the IEEE/CVF Conference on Computer Vision and Pattern Recognition. pp. 294–302 (2021)
21. Tabelini, L., Berriel, R., Paixao, T.M., Badue, C., De Souza, A.F., Oliveira-Santos, T.: Polylanenet: Lane estimation via deep polynomial regression. In: 2020 25th International Conference on Pattern Recognition (ICPR). pp. 6150–6156. IEEE (2021)
22. TuSimple: Tusimple benchmark. <https://github.com/TuSimple/tusimple-benchmark/> (Accessed September, 2020)
23. Weng, W., Wei, M., Ren, J., Shen, F.: Enhancing aerial object detection with selective frequency interaction network. IEEE Transactions on Artificial Intelligence **1**(01), 1–12 (2024)
24. Xu, H., Wang, S., Cai, X., Zhang, W., Liang, X., Li, Z.: Curvelane-nas: Unifying lane-sensitive architecture search and adaptive point blending. In: Computer Vision–ECCV 2020: 16th European Conference, Glasgow, UK, August 23–28, 2020, Proceedings, Part XV 16. pp. 689–704. Springer (2020)
25. Yoo, S., Lee, H.S., Myeong, H., Yun, S., Park, H., Cho, J., Kim, D.H.: End-to-end lane marker detection via row-wise classification. In: Proceedings of the IEEE/CVF Conference on Computer Vision and Pattern Recognition Workshops. pp. 1006–1007 (2020)
26. Yu, F., Wang, D., Shelhamer, E., Darrell, T.: Deep layer aggregation. In: Proceedings of the IEEE conference on computer vision and pattern recognition. pp. 2403–2412 (2018)
27. Zheng, T., Fang, H., Zhang, Y., Tang, W., Yang, Z., Liu, H., Cai, D.: Resa: Recurrent feature-shift aggregator for lane detection. In: Proceedings of the AAAI Conference on Artificial Intelligence. vol. 35, pp. 3547–3554 (2021)